

RESEARCH ARTICLE

The effects of superparamagnetic iron oxide nanoparticle exposure on gene expression patterns in the neural stem cells under magnetic field

Dan Li¹ and Ming-Liang Tang^{2*}

¹School of Biology, Food and Environment, Hefei University, Hefei, China; ²Department of Cardiovascular Surgery of the First Affiliated Hospital & Institute for Cardiovascular Science, Medical College, Soochow University, Suzhou, China

Abstract

Background: Due to the excellent reliable traceability and superparamagnetic properties, superparamagnetic iron oxide nanoparticles (SPIOs) are widely used for the applications in the field of biomedicine, including tissue engineering and regenerative medicine. However, the regulation of SPIOs on the gene expressions in the stem cells is not clear.

Methods: In this study, by RNA-Seq analysis, we analyzed the gene expression pattern in the neural stem cells (NSCs) treated with SPIOs in the presence or absence of static magnetic field (SMF).

Results: It was found that SPIOs with SMF regulated more gene expression in NSCs, while most of these genes have been previously reported to play a crucial role in NSCs fate decision.

Conclusions: Our findings reveal the ability of SPIOs and SMF in the regulation of gene expression in NSCs, which may provide an experimental basis for its applications.

Keywords: *SPIOs; stem cells; genes; SMF*

Received: 4 December 2021; Revised: 12 December 2021; Accepted: 13 December 2021; Published: 7 January 2022

Introduction

As nanoparticles display remarkable magnetic responsiveness, the diameter of superparamagnetic nanoparticles is generally less than 30 nm. Superparamagnetic iron oxide nanoparticles (SPIOs) are one kind of superparamagnetic nanoparticles that are widely reported for the applications in the field of biomedicine due to their high stability, good biological compatibility (1), and excellent superparamagnetism under magnetic fields (MFs) (2, 3). Specifically, SPIOs are demonstrated to regulate stem cell behaviors, including cell proliferation, directed differentiation and migration (4). The abovementioned ability indicates that SPIOs could be used in the regenerative medicine and tissue engineering. For example, a study in human mesenchymal stem cells showed that SPIOs successfully increased stem cell proliferation via accelerating cell cycle progression and diminishing intracellular oxidative stress (5). Another study found that osteogenesis of human bone-derived mesenchymal stem cells was promoted by SPIOs (6). Similar findings were reported in another study where osteogenic differentiation of adipose-derived

mesenchymal stem cells was boosted (7). The current reports clearly highlight the potential of SPIOs in the regulation of stem cell behaviors. As magnetic responsiveness biomaterial, it is inevitable to consider the cell behaviors under MFs. In fact, MFs have been proved to regulate cell proliferation in the last century (8). They can also control the stem cell differentiation, for instance, to osteoclasts (9) and osteoblasts and cartilage (10). Importantly, when co-treated with magnetic nanomaterials and MFs, cell behaviors were expectably affected. For example, they can facilitate drug delivery (11) and guide the growth direction of neurons (12). Thus, to understand the mechanisms of the regulation of SPIO in neural stem cells (NSCs) under the presence of MFs, we explored the gene expression pattern in the NSCs when treated with SPIO and MFs.

Methods

SPIOs synthesis

Classic chemical co-precipitation methods were employed to synthesize the SPIOs in the study, which was described

previously (13). In brief, 10 mL aqueous solution of polyglucose sorbitol carboxymethyl ether (200 mg) was aerated with nitrogen for 6 min to remove oxygen. Then, FeCl_2 and FeCl_3 were dissolved in deionized water, and the reaction mixture was added to the polyglucose sorbitol carboxymethyl solution. Subsequently, ammonium hydroxide (1 g, 28% w/v) was added to the mixed solution and stirred in a water bath for 30 min. at 80°C. Finally, the nanoparticles were collected using an ultrafiltration centrifuge tube and washed with ultrapure water for couple of times.

NSCs isolation and culture

Neural stem cells, isolated from the mouse hippocampus, were maintained in the DMEM-F12 medium (Gibco, Grand Island, NY) supplemented with B-27 (2%, Gibco), streptomycin (100 µg/mL, Sigma, St. Louis, MO) and penicillin (100 U/mL, Sigma) under the conditions of 5% CO_2 at 37°C. Cells were passed every 3 days. The cells at passages 5–10 were used for the subsequent experiments. The NSCs were treated with 300 µg/mL SPIOs with or without static magnetic field (SMF) (100 ± 10 mT) for 3 days. Animal studies were approved by the Care and Use of Animals Committee of Southeast University.

RNA extraction for RNA-Seq analysis

The cells were washed twice with phosphate-buffered saline and harvested with accutase. RNeasy mini kit (Qiagen, Valencia, CA) was used for isolating total RNA from the cells. Firstly, TruSeq™ RNA sample preparation kit (Illumina)

was applied to synthesize the paired-end libraries. The first-strand cDNA was synthesized using reverse transcriptase and random primers, and then second-strand cDNA was synthesized using DNA Polymerase I and RNase H. Following an end repair process, these cDNA fragments were purified and enriched with polymerase chain reaction (PCR) to create the final cDNA library. The purified libraries were quantified through Qubit® 2.0 Fluorometer (Life Technologies, Pleasanton, CA) and validated by Agilent 2100 bioanalyzer (Agilent Technologies, Santa Clara, CA) to calculate the mole concentration. Finally, clusters were generated by cBot with the library diluted to 10 pM and then were sequenced on the Illumina NovaSeq 6000 (Illumina). The library construction and sequencing were performed at Shanghai Sinomics Corporation.

Results

Global gene expression profile analysis

The differences in transcript expression levels were compared between the negative control group, the SPIOs incubation group (300 µg/mL) (SPIOs group), the SMF (100 ± 10 mT) group and the combined treated group of SMF (100 ± 10 mT) SPIOs (300 µg/mL) (SMF + SPIOs group). The NSCs in all groups were cultured for 3 days before gene expression profile by microarray assay. SMF treatment induced the medium number of significant differences in gene expression (total number is 1136,

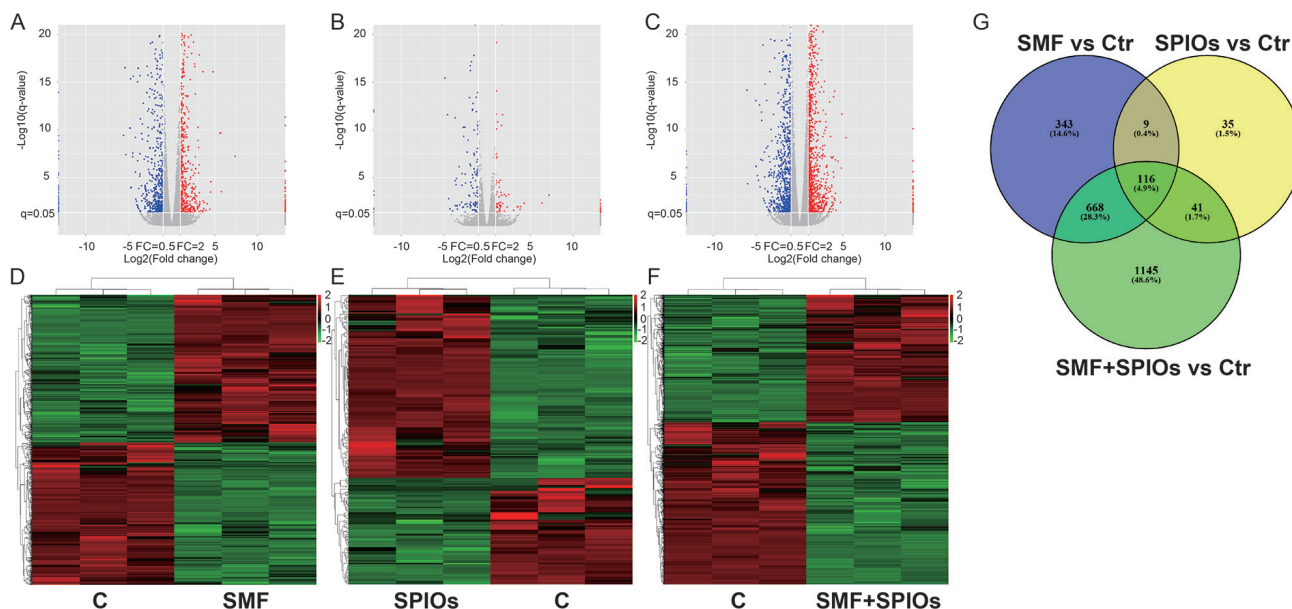


Fig. 1. Differentially expressed gene analysis. Volcano plots of different expressed genes of SMF versus control group (A), SPIOs versus control group (B), the SMF + SPIOs versus control group (C). Red dots represent the differentially expressed genes of the up-regulated expression, the blue dots represent the differentially expressed genes of the down-regulated expression, and the gray dots represent the genes that have no obvious differential expression. Heat map to differentially expressed gene of the SMF versus control group (D), SPIOs versus control group (E), the SMF + SPIOs versus control group (F). (G) Venn diagram of differentially expressed gene in different groups.

558 up-regulated genes and 578 down-regulated genes) (Fig. 1A and D). The significant differences in gene expression were observed in the NSCs treated with 300 mg/mL SPIOs, with at least 201 genes (127 up-regulated genes and 74 down-regulated genes) (Fig. 1B and E). Moreover, 1104 up-regulated genes and 866 down-regulated genes were detected under co-treatment group (Fig. 1C and 1), which had the most significant differences gene. In addition, Venn diagrams were shown to present the connections between the different genes in each experimental group (Fig. 1G). The differentially expressed genes in the SMF group compared with the SPIOs group had 125 identical differentially expressed genes, which accounted for 57.1 and 96.8% of the total differential genes in each group. The differentially expressed genes in the SMF versus control group compared with the SMF + SPIOs group versus control group had 784 differentially expressed genes, which accounted for 85 and 50.3% of the total differential genes in each group. The experimental group co-incubated with SPIOs versus control compared with the simultaneous SMF + SPIOs group versus control group had 159 differentially expressed genes, accounting for 98.1 and 23.1% of the total differential genes of each group, respectively.

Differentially expressed genes

The most abundantly expressed genes of NSCs were explored to characterize the gene expression profiles in NSCs in these three experimental groups. The expression levels for the top 200 most abundant genes were analyzed and compared with the control group (Fig. 2A–C). It was indicated that the majority of the transcripts that were highly expressed in SPIOs, SMF and SMF + SPIOs group were also abundantly expressed in the control group. Although the most abundantly expressed genes, such as *Gfap*, *Gh1*, *Slc25a18*, *Oat*, *Sms-ps*, *spry2*, *Car2*, and *Csrp1*, were significantly highly expressed in the SMF group, *Ftl1-ps1*, *Sms-ps* were significantly highly expressed in the SPIOs group and *Gfap*, *Ftl1-ps1*, *Sms-ps*, and *Mrps6* were significantly highly expressed in the SMF + SPIOs group.

Furthermore, the expression levels of all of the transcripts were compared, and the top 40 significant differentially expressed genes were located (Fig. 3). It was shown that the differentially expressed genes *Ptgs1*, *Cldn5*, *Dlx2*, *Spr1a*, *3100003L05Rik*, *Hnrnpa3*, etc. were uniquely expressed in the SMF group (Fig. 3A). The differentially expressed genes *Cldn5*, *Hnrnpa3*, *Dlx2*, *3100003L05Rik*, *Npr1*, etc. were only expressed in the SPIOs group (Fig. 3B), while the differentially expressed genes *Cldn5*, *C2cd4b*, *Dlx2*, *3100003L05Rik*, *H2ac10*, *Sulf1*, etc. were only expressed in the SMF + SPIOs group (Fig. 3C). However, *Bmp4*, *Lrrc75b*, *Dpp10* (Fig. 3D), *Zbtb6*, *Hspal1a* (Fig. 3E), *Gsg11*, *Kcnc4*, *Nog*,

Egr3 *Arhgdig* (Fig. 3F), etc. were only expressed in the control group.

Cell cycle analysis

The expression of genes regulating cell cycle and proliferation was further studied. It was found that *Gfap*, *Gem*, *Dusp1*, *Mmp2*, and *Slpr3* were significantly highly expressed in SMF groups (Fig. 4A), and that *Bmp4*, *Nog*, *Prkcq*, *Brin1*, *Txnip*, *Pdgfra*, *Id2*, *Igfbp5*, and *Rgcc* were significantly highly expressed in control groups (Fig. 4A). The highly expressed genes in SPIOs groups included *Ccnd3*, *Nupr1*, *Dusp1*, and *Mmp2* (Fig. 4B). In the SMF + SPIOs group, the highly expressed genes included *Nupr1*, *Mmp2*, *Slpr3*, *Ccnd3*, *Gem*, *Mycn*, *Dusp1*, *Apc*, *Atf4*, *Adamts1*, *Phlda1*, and *Sfrp1* (Fig. 4C). However, there were most highly expressed genes in the control group compared with the SMF + SPIOs group (Fig. 4D), including *Id3*, *Bmp4*, *Igfbp5*, *Rgcc*, *Mt1*, *Id4*, *Ccnb2*, *Egr1*, *Id2*, *Pdgfra*, and *Mmp2*.

Transcription factors analysis

TFs are taken as a specific element that can recognize particular DNA sequences to direct chromatin and transcription and form a complex system that guides expression of the genome. We found 26 significantly differentially expressed TFs in SMF and control groups ($P < 0.05$, fold change > 1). Among these genes, *Dlx2*, *Sox7*, *Cebpd*, *Zfp180*, *Zfp629*, *Otx1*, *Ets2*, *Tead2*, and *Zfp740* were significantly highly expressed in SMF groups, and *Sox8*, *Id2*, *Hes5*, *Zfp292*, *Id1*, *Id4*, *Nkx2-2*, *Sox10*, *Zfp488*, and *Myrf* were significantly highly expressed in control groups (Fig. 5A). *Sox7*, *Csdc2*, *Usf3*, *Zfp180*, *Zfp28*, and *Erg3* were significantly highly expressed in SPIOs groups, while none of those genes have been previously reported in function with NSCs. In contrast, *Hopx*, *Zbtb6* were significantly highly expressed in control groups (Fig. 5B). The highly expressed TF genes in the SMF + SPIOs group included *Dlx2*, *Sox7*, *Cebpd*, *Mycn*, *Usf3*, *Klf4*, *Zfp180*, *Pou3f1*, and *Rxra*. In the control group, the highly expressed TFs genes included *Id4*, *Egr1*, *Hopx*, *Hes5*, *Id1*, *Id2*, *Id3*, *Sox10*, *Zfp292*, *Hmgb3*, *Zfp488*, *Klf10*, etc.

Signaling pathway analysis

The fate of stem cells is regulated by a variety of signaling pathways, including Wnt, Hippo, MAPK pathways, etc. The balance of NSCs is regulated by WNT, Notch, FGF, and BMP signaling cascades (14, 15). In this study, we explored which signaling pathway is affected by SPIO and SMF treatment. As shown in Fig. 6A, we found 26 signaling pathways of differentially expressed gene enrichment. Among these, there were more up-regulated genes than down-regulated genes, especially *Fzd8*, *Gsn*, *Dusp1*, and *Cacng5* had higher expression. In Fig. 6B, there were 21 signaling pathways of differential expressed

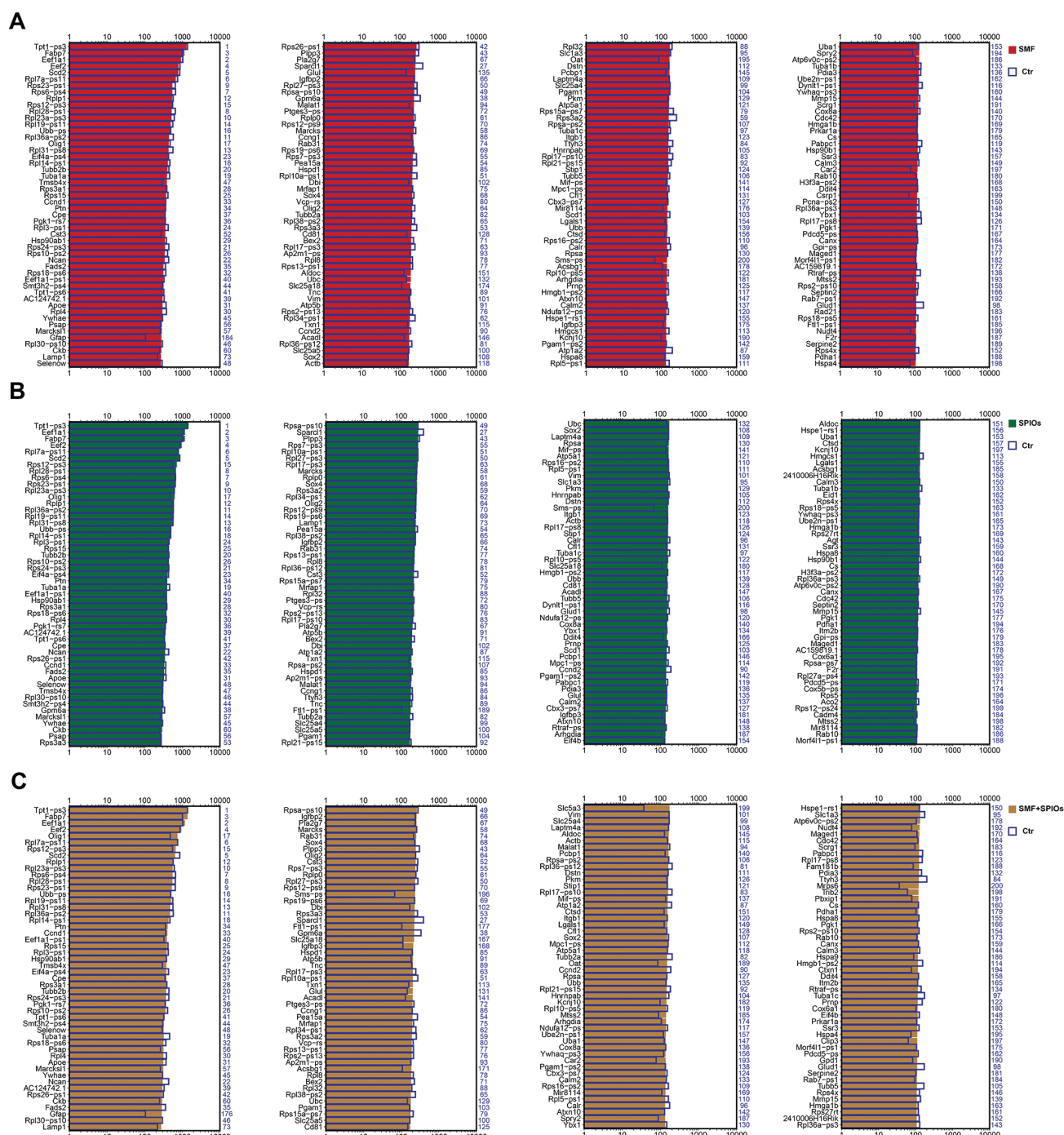


Fig. 2. Highly expressed genes in different groups. The top 200 highly expressed genes of the SMF group (red bar) (A), SPIOs group (green bar) (B), the SMF+SPIOs group ranked in descending order (yellow bar) (C). The number in blue on the right side of each panel represents the same gene ranking in the control group.

gene enrichment, and the nitrogen metabolism had the maximum enrichment factor. Among these, the number of up-regulated genes was more than the down-regulated genes, but the differential expression of genes was low. There were 52 signaling pathways of differentially expressed gene enrichment in the SMF + SPIOs group compared with the control group, and there were more

up-regulated genes than down-regulated genes in six main signaling pathways (Fig. 6C). Among these, Fzd8, Gsn, and Dusp1 showed higher expression.

Discussion

In this study, SPIOs, SMF, or SMF+SPIOs could induce differentially expressed genes in NSCs. In

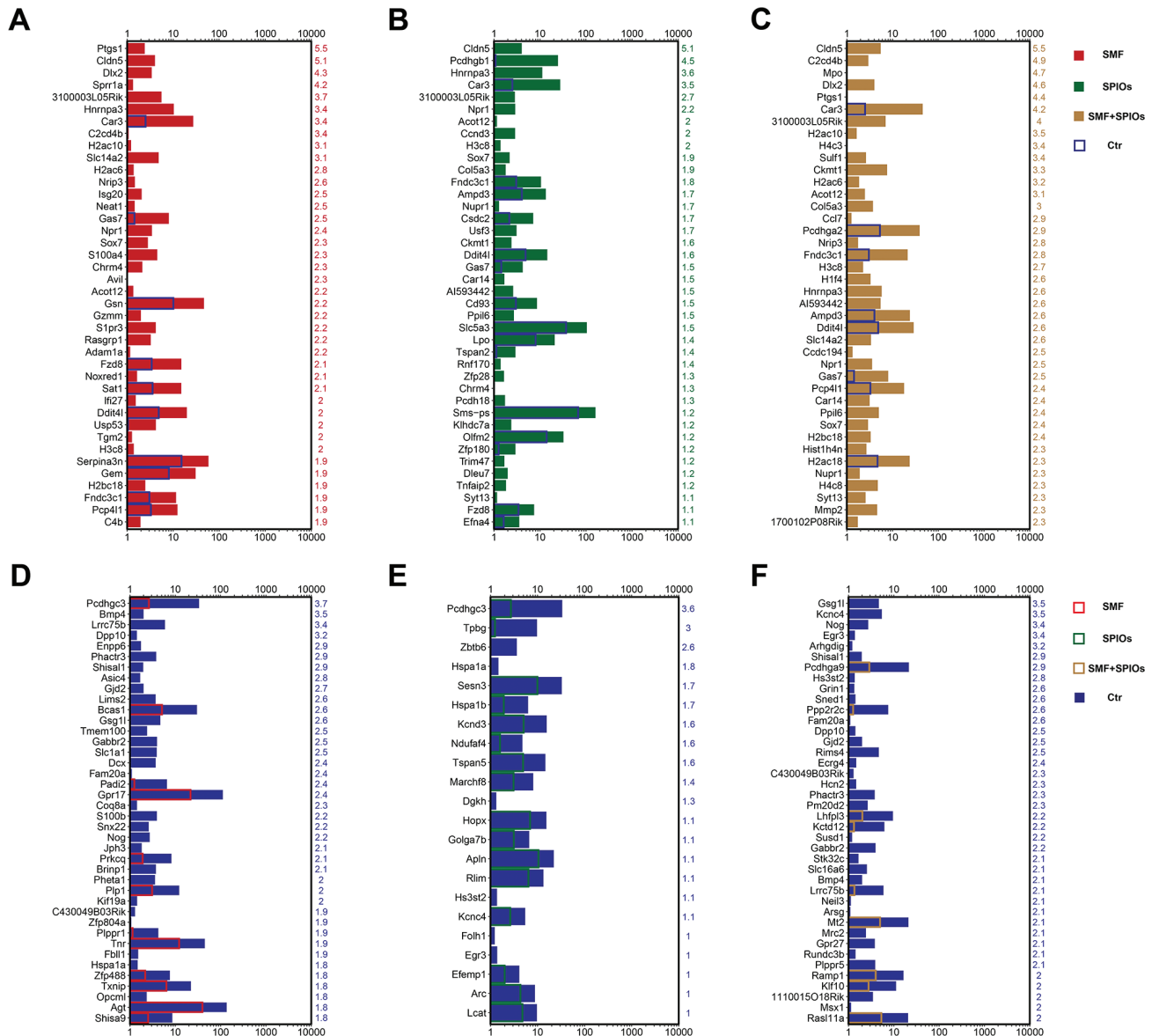


Fig. 3. The differentially expressed genes of NSCs in different experimental groups. The top 40 highly differentially expressed genes of NSCs cultured in the SMF group (A), SPIOs group (B), and the SMF + SPIOs group ranked in descending order (C). The number on the right of each panel represents the fold difference in expression for NSCs in different culture condition groups versus control group. (D-F) The top 40 highly differentially expressed genes of NSCs in the control group ranked in descending order. The number on the right of each panel represents the fold difference in expression for NSCs in the control group versus different culture condition groups.

transcriptome analyses, the top 200 highly expressed genes, differentially expressed genes, cell cycle-related genes, TF genes, and several signaling pathways were included.

Most of those genes have been reported to be involved in the stem cells fate decisions, specifically in NSCs. Notably, electrical stimulation might promote the expression of *Mmp2* to accelerate neurite regeneration in cultured ganglion neurons (16). The effects of *BMP4* have been observed in the proliferation and differentiation of NSCs. Recently, *BMP4* was reported to inhibit the proliferation

of monkey-derived NSCs via the Smad signaling pathway (17). Meanwhile, *BMP4*/LIF has the potential to promote the differentiation of monkey-derived NSCs by regulating Notch signaling (17). *Brinp1* family member including *Brinp1* was previously reported to suppress the process of cell cycle and induce the differentiation of embryonic stem cell-derived NSCs (18). *Pdgfra* could deregulate self-renewal, differentiation, and survival of NSCs in embryonic brains (19). *Myc* family was proved to be a critical transcription factor in the self-renewal division of many types of stem cells (20). For example, N-Myc is necessary

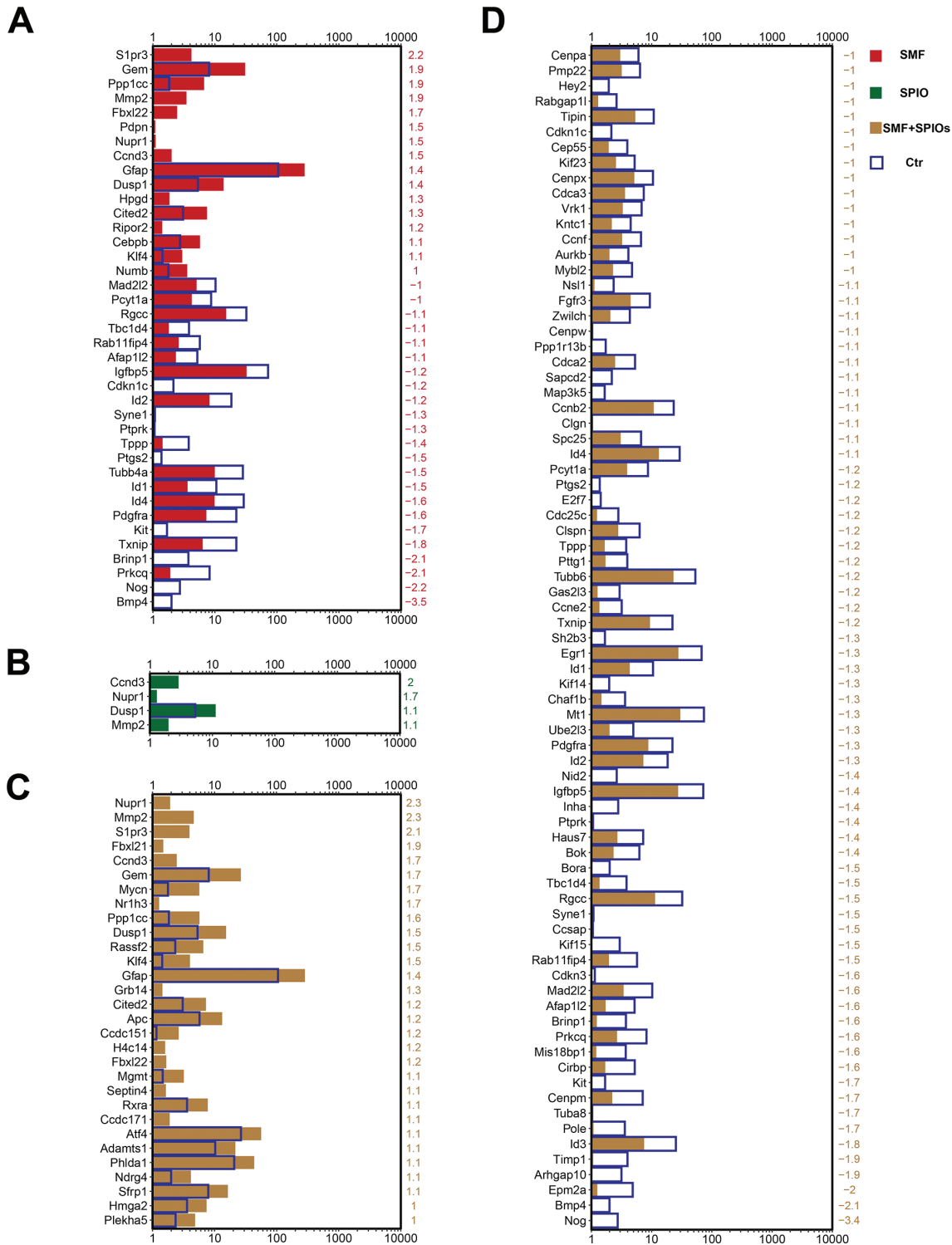


Fig. 4. Cell cycle-related differentially expressed genes of NSCs in the SMF group (A), SPIOs group (B), the SMF + SPIOs group (C), and control group (D).

for normal neurogenesis and regulate the proliferation and differentiation of NPCs (21). *Atf4* gene encoded transcription factor ATF4, which connected with endoplasmic reticulum (ER)-stress. ER stress can be caused by the

accumulation of misfolded/unfolded proteins and induces the unfolded protein response (UPR), which have adverse effects on self-renewal and differentiation of NSCs (22). While *Ccnb2* (cyclin B2) works mainly through regulating

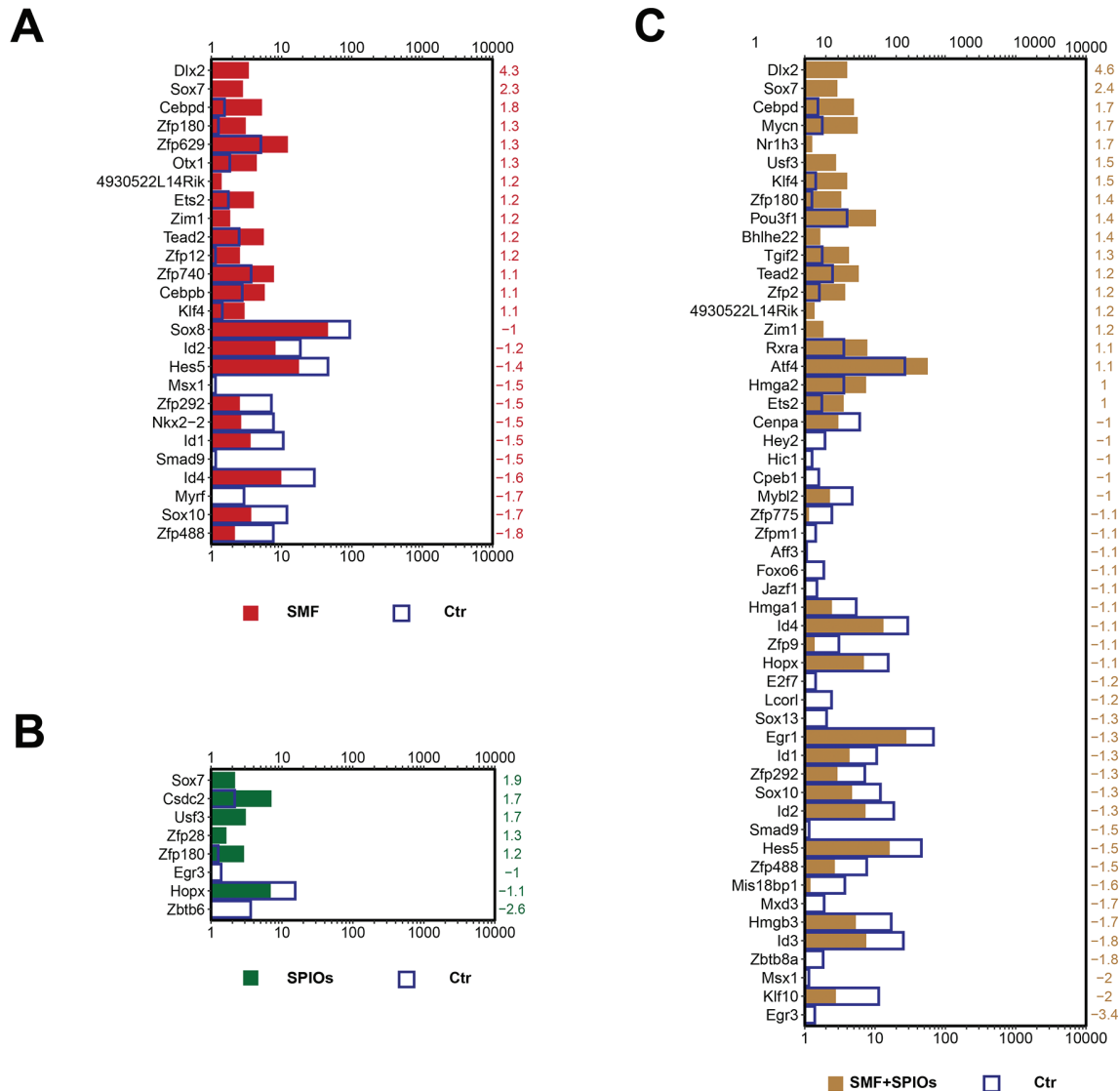


Fig. 5. Transcription factors of NSCs in different culture condition groups. (A) The expression of 26 genes involved in the transcription factor of NSCs cultured in SMF group and control group. (B) The expression of eight genes involved in the transcription factor of NSCs cultured in the SPIOs group and control group. (C) The expression of 52 genes involved in the transcription factor of NSCs cultured in the SMF + SPIOs group and control group.

the G_2/M and plays a crucial role in cell proliferation (23). *Otx1* is generally connected with the development of the central nervous system and acts as a homeobox-containing transcription factor (24). In addition, the expression of *Otx1* has been demonstrated to determine the number of neurons (25). Recently, *Otx1* is also identified as a key element to regulate the proliferation and differentiation of cortical progenitors (26). The Krüppel-like transcription factor (KLF) families are previously reported to regulate a diverse array of cellular processes, including development, differentiation, proliferation, and apoptosis (27). Especially, *Klf4* has been demonstrated as a key factor in regulating NSC proliferation and differentiation (28).

Pou3f1 is also taken as an important TF promoting neural fate (29). However, in contrast with the SMF group, the control group also included common TFs in determining the fate of NSCs. *Sox10* belongs to a member of Sox E family, which has a close relationship with the differentiation of NSCs (30). The previous report suggested that the regulatory mechanism of oligodendrocyte specification and differentiation from NSCs or neural progenitor cells (NPCs) is through the transcription factors *Nkx2.2* and *Sox10* (31). In addition, *Nkx2.2* has shown a similar function during ESC-derived NSC differentiation into oligodendrocytes (32). *Zfp488* plays an important role in the development of oligodendrocyte lineage cells and

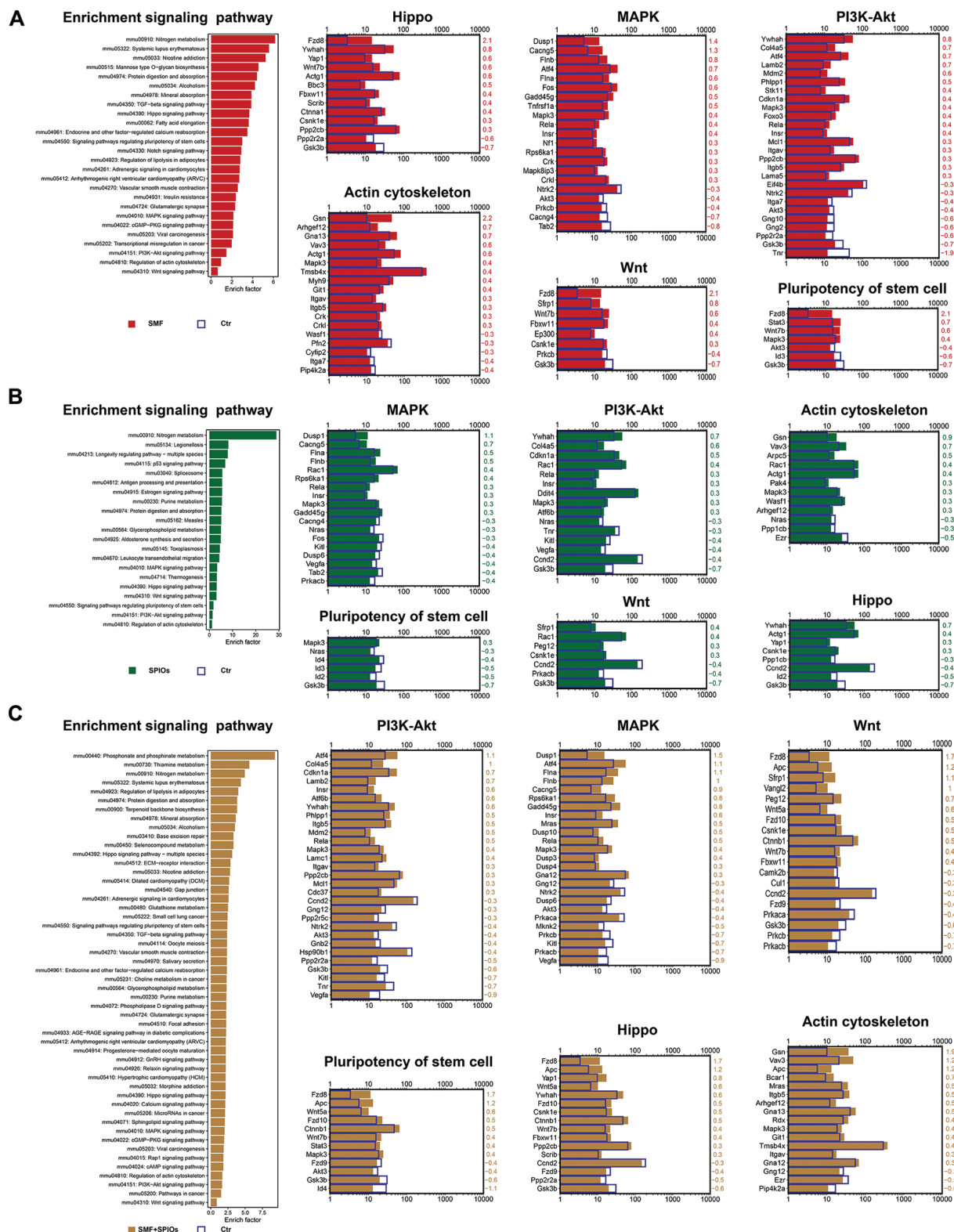


Fig. 6 Signaling pathway gene expressions of NSCs in different culture condition groups. (A) The differential KEGG pathways from NSCs cultured in the SMF group versus NSCs of control. (B) The differential KEGG pathways from NSCs cultured in SPIOs group versus NSCs of control; (C) The differential KEGG pathways from NSCs cultured in the SMF and co-incubated with SPIOs group versus NSCs of control. The red bars represent the gene expression levels of NSCs cultured in the SMF group. The green bars represent the gene expression levels of NSCs cultured in the SPIOs group. The yellow bars represent the gene expression levels of NSCs cultured in the SMF + SPIOs group. The blue bars represent the gene expression levels of NSCs cultured in the control group.

differentiation of oligodendrocyte progenitor cells (33, 34), and the expression of *Zfp488* selectively directed the fate of NSCs toward generating functional oligodendrocytes (35). In a previous study, it was found that *Id1*, *Id2*, and *Id3* elevated self-renewing and proliferation abilities of NSCs while inhibiting neuronal differentiation (36). Meanwhile, *Id2* and *Id4* play a critical role in regulating the process of cell cycle by inhibiting the effects of related proteins (37).

We also explored the actin cytoskeleton signaling pathway. According to previous reports, the actin cytoskeleton-dependent forces are necessary for various cell behaviors, including cell migration, interaction with the cell microenvironment, cell shapes and mechanical properties of the cell surface (38). However, there are few reports focusing on the direct regulation of NSC behaviors by actin cytoskeleton-dependent forces, which deserves an in-depth investigation in the future.

Conflict of interest and funding

This research work was supported by grants from the Major State Basic Research Development Program of China (973 Program).

References

- Hawket BS. Monodispersed polymer encapsulated superparamagnetic iron oxide nanoparticles for cell labeling. *Polymer*. 2016; 106(5): 238–248.
- Andreu I, Natividad E, Solozabal L, Roubeau O. Nano-objects for addressing the control of nanoparticle arrangement and performance in magnetic hyperthermia. *ACS Nano*. 2015; 9(2): 1408–19. doi: 10.1021/nn505781f
- Mashhadi Malekzadeh A, Ramazani A, Tabatabaei Rezaei SJ, Niknejad H. Design and construction of multifunctional hyperbranched polymers coated magnetite nanoparticles for both targeting magnetic resonance imaging and cancer therapy. *J Colloid Interface Sci*. 2017; 490: 64–73. doi: 10.1016/j.jcis.2016.11.014
- Wei H, Hu Y, Wang J, Gao X, Qian X, Tang M. Superparamagnetic iron oxide nanoparticles: cytotoxicity, metabolism, and cellular behavior in biomedicine applications. *Int J Nanomed* 2021; 16: 6097–113. doi: 10.2147/IJN.S321984
- Huang DM, Hsiao JK, Chen YC, Chien LY, Yao M, Chen YK, et al. The promotion of human mesenchymal stem cell proliferation by superparamagnetic iron oxide nanoparticles. *Biomaterials* 2009; 30(22): 3645–51. doi: 10.1016/j.biomaterials.2009.03.032
- Wang QW, Chen B, Cao M, Sun JF, Wu H, Zhao P, et al. Response of MAPK pathway to iron oxide nanoparticles in vitro treatment promotes osteogenic differentiation of hBMSCs. *Biomaterials*. 2016; 86: 11–20. doi: 10.1016/j.biomaterials.2016.02.004
- Xiao HT, Wang L, Yu B. Superparamagnetic iron oxide promotes osteogenic differentiation of rat adipose-derived stem cells. *Int J Clin Exp Med*. 2015; 8(1): 698–705. doi: 10.1096/fasebj.13.1.95
- Fanelli C, Coppola S, Barone R, Colussi C, Gualandi G, Volpe P, et al. Magnetic fields increase cell survival by inhibiting apoptosis via modulation of Ca²⁺ influx. *FASEB J* 1999; 13(1): 95–102. doi: 10.1096/fasebj.13.1.95
- Kang KS, Hong JM, Kang JA, Rhie JW, Jeong YH, Cho DW. Regulation of osteogenic differentiation of human adipose-derived stem cells by controlling electromagnetic field conditions. *Exp Mol Med*. 2013; 45: e6. doi: 10.1038/emm.2013.11
- Ross CL, Siriwardane M, Almeida-Porada G, Porada CD, Brink P, Christ GJ, et al. The effect of low-frequency electromagnetic field on human bone marrow stem/progenitor cell differentiation. *Stem Cell Res* 2015; 15(1): 96–108. doi: 10.1016/j.scr.2015.04.009
- Qiu Y, Tong S, Zhang L, Sakurai Y, Myers DR, Hong L, et al. Magnetic forces enable controlled drug delivery by disrupting endothelial cell-cell junctions. *Nat Commun*. 2017; 8: 15594. doi: 10.1038/ncomms15594
- Riggio C, Calatayud MP, Giannaccini M, Sanz B, Torres TE, Fernandez-Pacheco R, et al. The orientation of the neuronal growth process can be directed via magnetic nanoparticles under an applied magnetic field. *Nanomed-Nanotechnol*. 2014; 10(7): 1549–58. doi: 10.1016/j.nano.2013.12.008
- Wang P, Ma S, Ning G, Chen W, Wang B, Ye D, et al. Entry-prohibited effect of kHz pulsed magnetic field upon interaction between SPIO nanoparticles and mesenchymal stem cells. *IEEE Trans Biomed Eng* 2020; 67(4): 1152–8. doi: 10.1109/TBME.2019.2931774
- Israsena N, Hu M, Fu W, Kan L, Kessler JA. The presence of FGF2 signaling determines whether beta-catenin exerts effects on proliferation or neuronal differentiation of neural stem cells. *Dev Biol* 2004; 268(1): 220–31. doi: 10.1016/j.ydbio.2003.12.024
- Akai J, Halley PA, Storey KG. FGF-dependent Notch signaling maintains the spinal cord stem zone. *Genes Dev*. 2005; 19(23): 2877–87. doi: 10.1101/gad.357705
- Han S, Kim DH, Sung J, Yang H, Park JW, Youn I. Electrical stimulation accelerates neurite regeneration in axotomized dorsal root ganglion neurons by increasing MMP-2 expression. *Biochem Biophys Res Commun* 2019; 508(2): 348–53. doi: 10.1016/j.bbrc.2018.11.159
- Wang M, Yu L, Zhu LY, He H, Ren J, Pan J, et al. Cytokines induce monkey neural stem cell differentiation through Notch signaling. *Biomed Res Int* 2020; 2020: 1308526. doi: 10.1155/2020/1308526
- Terashima M, Kobayashi M, Motomiya M, Inoue N, Yoshida T, Okano H, et al. Analysis of the expression and function of BRINP family genes during neuronal differentiation in mouse embryonic stem cell-derived neural stem cells. *J Neurosci Res* 2010; 88(7): 1387–93. doi: 10.1002/jnr.22315
- Li B, Yi P, Zhang B, Xu C, Liu Q, Pi Z, et al. Differences in endoplasmic reticulum stress signalling kinetics determine cell survival outcome through activation of MKP-1. *Cell Signal* 2011; 23(1): 35–45. doi: 10.1016/j.cellsig.2010.07.019
- Laurenti E, Wilson A, Trumpp A. Myc's other life: stem cells and beyond. *Curr Opin Cell Biol* 2009; 21(6): 844–54. doi: 10.1016/j.ceb.2009.09.006
- Knoepfler PS, Cheng PF, Eisenman RN. N-myc is essential during neurogenesis for the rapid expansion of progenitor cell populations and the inhibition of neuronal differentiation. *Genes Dev* 2002; 16(20): 2699–712. doi: 10.1101/gad.1021202
- Mansouri S, Agartz I, Ogren SO, Patrone C, Lundberg M. PACAP protects adult neural stem cells from the neurotoxic effect of ketamine associated with decreased apoptosis, ER stress and mTOR pathway activation. *PLoS One* 2017; 12(1): e0170496. doi: 10.1371/journal.pone.0170496

23. Wu T, Zhang X, Huang X, Yang Y, Hua X. Regulation of cyclin B2 expression and cell cycle G2/m transition by menin. *J Biol Chem* 2010; 285(24): 18291–300. doi: 10.1074/jbc.M110.106575
24. Panto MR, Zappala A, Tuorto F, Cicirata F. Role of the Otx1 gene in cell differentiation of mammalian cortex. *Eur J Neurosci* 2004; 19(10): 2893–902. doi: 10.1111/j.0953-816X.2004.03326.x
25. Gao P, Postiglione MP, Krieger TG, Hernandez L, Wang C, Han Z, et al. Deterministic progenitor behavior and unitary production of neurons in the neocortex. *Cell* 2014; 159(4): 775–88. doi: 10.1016/j.cell.2014.10.027
26. Huang B, Li X, Tu X, Zhao W, Zhu D, Feng Y, et al. OTX1 regulates cell cycle progression of neural progenitors in the developing cerebral cortex. *J Biol Chem* 2018; 293(6): 2137–48. doi: 10.1074/jbc.RA117.001249
27. Bhattacharya R, Senbanerjee S, Lin Z, Mir S, Hamik A, Wang P, et al. Inhibition of vascular permeability factor/vascular endothelial growth factor-mediated angiogenesis by the Kruppel-like factor KLF2. *J Biol Chem* 2005; 280(32): 28848–51. doi: 10.1074/jbc.C500200200
28. Gao Y, Qiao H, Zhong T, Lu Z, Hou Y. MicroRNA29a promotes the neural differentiation of rat neural stem/progenitor cells by targeting KLF4. *Mol Med Rep* 2020; 22(2): 1008–16. doi: 10.3892/mmr.2020.11177
29. Song L, Sun N, Peng G, Chen J, Han JD, Jing N. Genome-wide ChIP-seq and RNA-seq analyses of Pou3f1 during mouse pluripotent stem cell neural fate commitment. *Genom Data*. 2015; 5: 375–7. doi: 10.1016/j.gdata.2015.06.028
30. Castelo-Branco G, Lilja T, Wallenborg K, Falcao AM, Marques SC, Gracias A, et al. Neural stem cell differentiation is dictated by distinct actions of nuclear receptor corepressors and histone deacetylases. *Stem Cell Rep*. 2014; 3(3): 502–15. doi: 10.1016/j.stemcr.2014.07.008
31. Rowitch DH. Glial specification in the vertebrate neural tube. *Nat Rev Neurosci*. 2004; 5(5): 409–19. doi: 10.1038/nrn1389
32. Stolt CC, Rehberg S, Ader M, Lommes P, Riethmacher D, Schachner M, et al. Terminal differentiation of myelin-forming oligodendrocytes depends on the transcription factor Sox10. *Genes Dev*. 2002; 16(2): 165–70. doi: 10.1101/gad.215802
33. Soundarapandian MM, Selvaraj V, Lo UG, Golub MS, Feldman DH, Pleasure DE, et al. Zfp488 promotes oligodendrocyte differentiation of neural progenitor cells in adult mice after demyelination. *Sci Rep*. 2011; 1: 2. doi: 10.1038/srep00002
34. Wang SZ, Dulin J, Wu H, Hurlock E, Lee SE, Jansson K, et al. An oligodendrocyte-specific zinc-finger transcription regulator cooperates with Olig2 to promote oligodendrocyte differentiation. *Development* 2006; 133(17): 3389–98. doi: 10.1242/dev.02522
35. Biswas S, Chung SH, Jiang P, Dehghan S, Deng W. Development of glial restricted human neural stem cells for oligodendrocyte differentiation in vitro and in vivo. *Sci Rep*. 2019; 9(1): 9013. doi: 10.1038/s41598-019-45247-3
36. Jung S, Park RH, Kim S, Jeon YJ, Ham DS, Jung MY, et al. Id proteins facilitate self-renewal and proliferation of neural stem cells. *Stem Cells Dev* 2010; 19(6): 831–41. doi: 10.1089/scd.2009.0093
37. Iavarone A, Garg P, Lasorella A, Hsu J, Israel MA. The helix-loop-helix protein Id-2 enhances cell proliferation and binds to the retinoblastoma protein. *Genes Dev* 1994; 8(11): 1270–84. doi: 10.1101/gad.8.11.1270
38. Svitkina T. The actin cytoskeleton and actin-based motility. *Cold Spring Harb Perspect Biol* 2018; 10(1): a018267. doi: 10.1101/cshperspect.a018267

***Ming-Liang Tang**

Department of Cardiovascular Surgery of the First Affiliated Hospital & Institute for Cardiovascular Science, Medical College, Soochow University, Suzhou, 215000, China
Email: mltang@suda.edu.cn